

Supporting Information for

**Field and dilution effects on the magnetic relaxation
behaviours of a 1D dysprosium(III)-carboxylate chain built
from chiral ligands**

Tian Han,^a Ji-Dong Leng,^a You-Song Ding,^a Yanyan Wang,^a Zhiping Zheng^{a,b}
and Yan-Zhen Zheng^{*,a}

^a *Center for Applied Chemical Research, Frontier Institute of Science and Technology, and
College of Science, Xi'an Jiaotong University, Xi'an 710054, China. Email:
zheng.yanzhen@mail.xjtu.edu.cn*

^b *Department of Chemistry, The University of Arizona, Tucson, Arizona 85721, USA.*

Experimental Section

All the starting materials were commercially available reagents for analytical grade and used without further purification.

{[Dy(L)₃(H₂O)]·5H₂O}_n (1): Dy(NO₃)₃·6H₂O (0.4 mmol) was added to a solution of water/acetonitrile (1:5, 6 ml) containing HL (0.4 mmol) and Et₃N (0.4 mmol). Then the solvent of water (4 ml) and acetonitrile (5 ml) was added to the mixture. After stirring for 10 min, the resultant solution was filtered and left to allow the slow evaporation of the solvent. Colorless needle-like single crystals suitable for X-ray diffraction analysis were obtained quickly after 1 day. Yield: 58 mg (51.5 %, based on the ligand). Elemental analysis (*calcd.* for C₂₁H₄₅DyO₂₄): C 29.88%, H 5.37%; found C 29.47%, H 5.62%.

{[Dy_{0.5}Y_{0.5}(L)₃(H₂O)]·5H₂O}_n (2): Compound **2** was prepared with the similar method to that of **1**, with only Dy(NO₃)₃·6H₂O/Y(NO₃)₃·6H₂O (1:1) instead of Dy(NO₃)₃·6H₂O.

X-ray crystallography and physical measurement

Single-crystal X-ray diffraction data of **1** and **2** were recorded on a Bruker Apex CCD II area-detector diffractometer with graphite-monochromated CuK α /MoK α radiation at 150 K/293 K. The structures were solved by direct method and refined by full-matrix least-squares method on F^2 with anisotropic thermal parameters for all non-hydrogen atom. Hydrogen atoms were located geometrically and refined isotropically.

Elemental analyses (C and H) were carried out on a Vario EL III elemental analyzer. Inductively coupled plasma (ICP) analysis was performed on a Perkin-Elmer Optima 3300DV spectrometer. The Powder X-ray diffraction (PXRD) measurements were recorded on a Rigaku Smartlab X-ray diffractometer. Direct-current (dc) magnetic susceptibilities were measured on a Quantum Design MPMS XL-7 SQUID magnetometer. Diamagnetic corrections were made with Pascal's constants for all the constituent atoms and sample holder. Alternating-current (ac) magnetic susceptibility data were collected on the same instrument employing a 3.5 Oe oscillating field at frequencies up to 1500 Hz. Measurement of the circular dichroism for **1** in the solid state was carried out with a JASCO 715 spectrometer on powder sample embedded in KBr pellet; the CD measurement for the ligand was carried out with a JASCO 815 spectrometer in an aqueous solution. Electric hysteresis loop was measured at room temperature by using a Radiant P-PMF instrument for **1** in a 0.15 cm thick pressed pellet.

Table S1. Crystallographic data and structure refinement for compound **1** at 150 K.

Compound	1
formula	C ₂₁ H ₄₅ DyO ₂₄
<i>M</i> /g mol ⁻¹	844.07
crystal system	Monoclinic
space group	<i>P</i> 2 ₁
<i>a</i> , Å	6.0848(2)
<i>b</i> , Å	25.2704(10)
<i>c</i> , Å	10.5635(4)
<i>α</i> , deg	90
<i>β</i> , deg	105.602(2)
<i>γ</i> , deg	90
<i>V</i> , Å ³	1564.45(10)
<i>Z</i>	2
<i>d</i> _{cal} /g cm ⁻³	1.792
temperature, K	150(2)
F(000)	858
<i>θ</i> range	3.50–68.32°
completeness	99.3 %
residual map, e Å ⁻³	0.506 and -0.849
Goodness-of-fit on <i>F</i> ²	0.926
final indices [<i>I</i> > 2σ(<i>I</i>)]	<i>R</i> ₁ = 0.0218, <i>wR</i> ₂ = 0.0465
<i>R</i> indices (all data)	<i>R</i> ₁ = 0.0225, <i>wR</i> ₂ = 0.0467
absolute structure parameter	0.014(2)

Table S2. Selected bonds and angles for **1**. Symmetry code: #1 *x*+1,*y*,*z*.

Bonds/Angles	Å / °	Bonds/Angles	Å / °
Dy1-O14	2.303(2)	O14-Dy1-O19	80.52(9)
Dy1-O2	2.314(2)	O2-Dy1-O19	77.84(7)
Dy1-O19	2.3559(18)	O14-Dy1-O9#1	77.45(9)
Dy1-O9#1	2.3578(15)	O2-Dy1-O9#1	74.38(7)
Dy1-O8	2.3623(17)	O19-Dy1-O8	78.99(7)
Dy1-O13	2.365(2)	O14-Dy1-O13	65.72(7)
Dy1-O1	2.373(2)	O9#1-Dy1-O13	89.43(9)
Dy1-O7#1	2.389(2)	O8-Dy1-O13	74.04(7)
O14-Dy1-O2	81.98(7)	O2-Dy1-O1	65.73(7)
O1-Dy1-O7#1	75.95(7)	O19-Dy1-O1	86.09(9)
O13-Dy1-O7#1	79.57(7)	O9#1-Dy1-O7#1	64.15(6)
O8-Dy1-O7#1	71.18(7)	O8-Dy1-O1	77.62(6)

Table S3. δ and φ values for compound **1**. Symmetry code: #1 $x+1,y,z$

1		DD	TP	SAP
δ_1	O2 [O1 O19] O8	45.1	29.5	0.0
δ_2	O14 [O19 O13] O8	24.9	29.5	21.8
δ_3	O2 [O1 O9#1] O7#1	17.5	29.5	48.2
δ_4	O14 [O13 O9#1] O7#1	34.8	29.5	48.2
φ_1	O1-O13-O2-O14	7.6	0	14.1
φ_2	O19-O9#1-O8-O7#1	10.4		24.5

A [B C] D is the dihedral angle between the ABC plane and the BCD plane. A-B-C-D is the dihedral angle between the (AB)CD plane and the AB(CD) where (AB) signifies the midpoint of the AB edge.

Table S4. Crystallographic data and structure refinement for compound **2**.

Compound	2
formula	$C_{42}H_{90}DyYO_{48}$
$M/g\ mol^{-1}$	1614.55
crystal system	Monoclinic
space group	$P2_1$
$a, \text{\AA}$	6.0796(2)
$b, \text{\AA}$	25.2483(7)
$c, \text{\AA}$	10.5544(3)
α, deg	90
β, deg	105.6740(10)
γ, deg	90
$V, \text{\AA}^3$	1559.85(8)
Z	1
$d_{cal}/g\ cm^{-3}$	1.719
temperature, K	150(2)
F(000)	831
θ range	1.61–25.01°
completeness	99.9 %
residual map, $e\ \text{\AA}^{-3}$	0.342 and –0.372
Goodness-of-fit on F^2	1.064
final indices [$I > 2\sigma(I)$]	$R_1 = 0.0142, wR_2 = 0.0361$
R indices (all data)	$R_1 = 0.0144, wR_2 = 0.0362$
absolute structure parameter	–0.016(3)

Table S5. Crystallographic data and structure refinement for compound **1** at room temperature.

compound	1
formula	C ₂₁ H ₄₅ DyO ₂₄
<i>M</i> /g mol ⁻¹	844.07
crystal system	Monoclinic
space group	<i>P</i> 2 ₁
<i>a</i> , Å	6.1041(11)
<i>b</i> , Å	25.365(4)
<i>c</i> , Å	10.5919(19)
<i>α</i> , deg	90
<i>β</i> , deg	105.114(2)
<i>γ</i> , deg	90
<i>V</i> , Å ³	1583.2(5)
<i>Z</i>	2
<i>d</i> _{cal} /g cm ⁻³	1.771
temperature, K	293(2)
F(000)	858
<i>θ</i> range	1.61–25.01°
completeness	98.7 %
residual map, e Å ⁻³	2.653 and -2.640
Goodness-of-fit on <i>F</i> ²	1.061
final indices [<i>I</i> >2σ(<i>I</i>)]	<i>R</i> ₁ = 0.0430, <i>wR</i> ₂ = 0.1041
<i>R</i> indices (all data)	<i>R</i> ₁ = 0.0455, <i>wR</i> ₂ = 0.1054
absolute structure parameter	0.028(16)

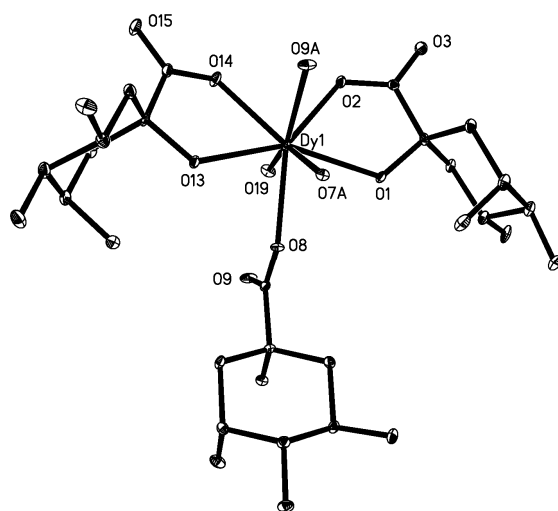


Fig. S1 Perspective view of asymmetric unit of **1**. H atoms are omitted for clarity.

Symmetry code: A $x+1,y,z$.

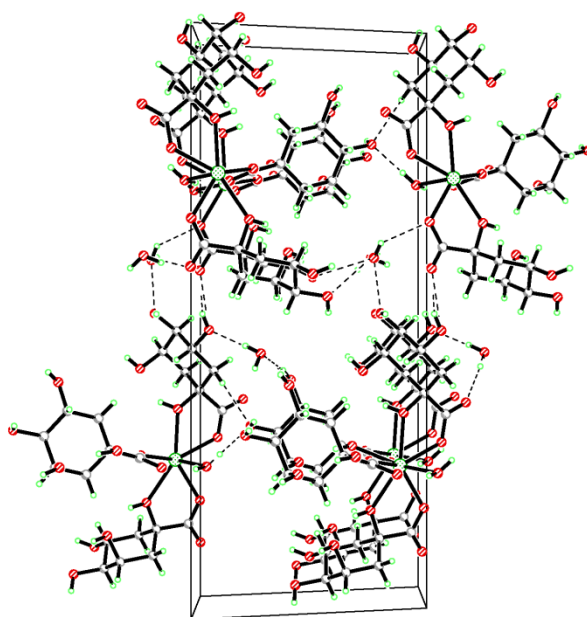


Fig. S2 The 3D supramolecular framework of **1** connected by hydrogen bonds.

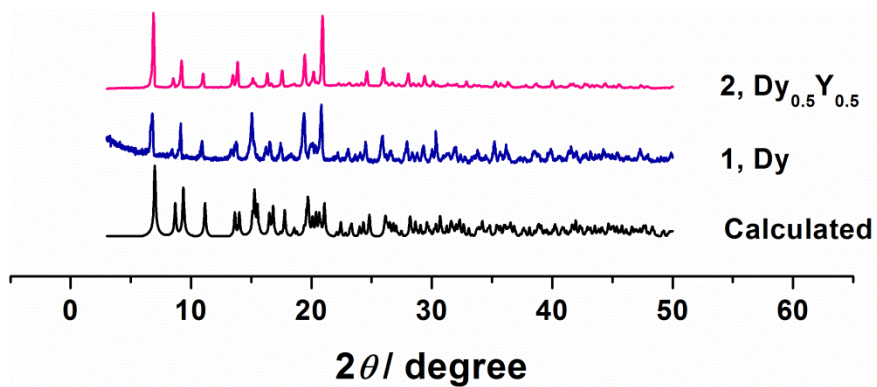


Fig. S3 The PXRD curves of **1** and **2**. The black curve is calculated from the single crystal data of **1**.

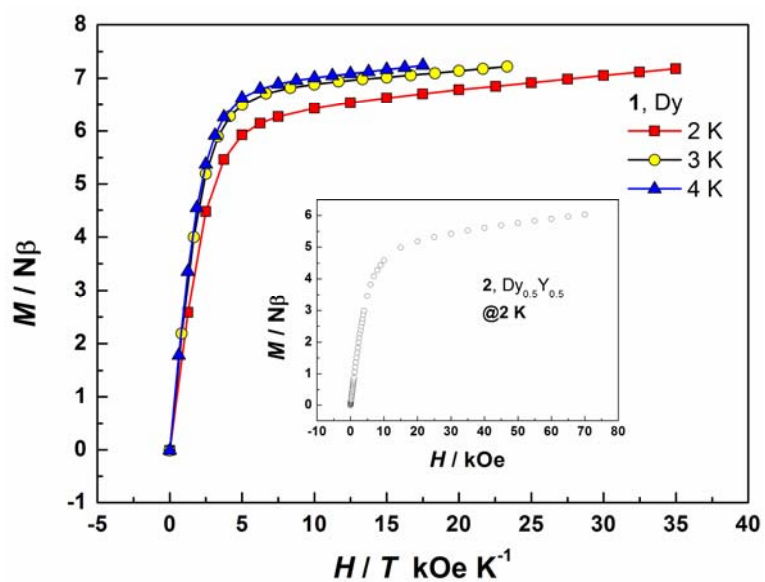


Fig. S4 $M/N\beta$ vs. HT^{-1} plots at various temperatures for **1**. The inset is the plot of M vs. H at 2 K for **2**.

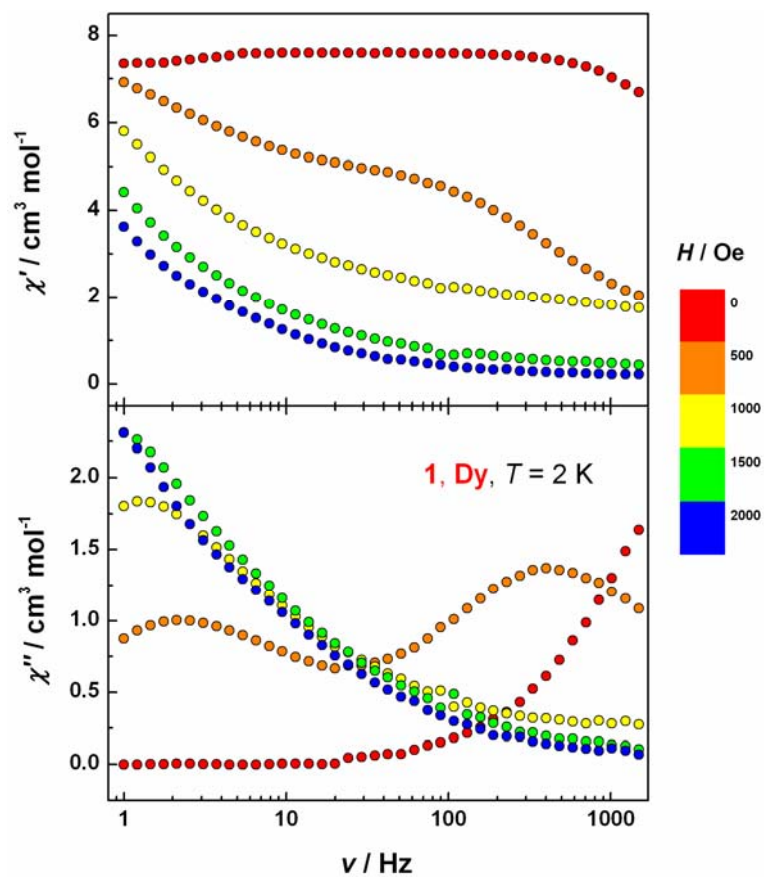


Fig. S5 Frequency dependence of the ac susceptibility for **1** at 2 K under various dc fields.

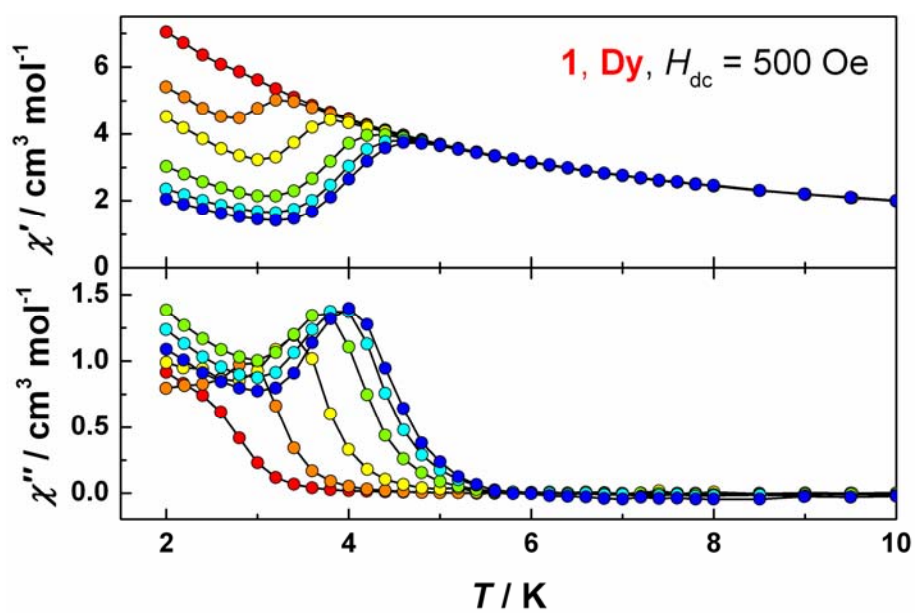


Fig. S6 Temperature dependence of the in-phase and out-of-phase ac susceptibility for **1** under 500 Oe dc field in range of 1 Hz (red) to 1500 Hz (blue).

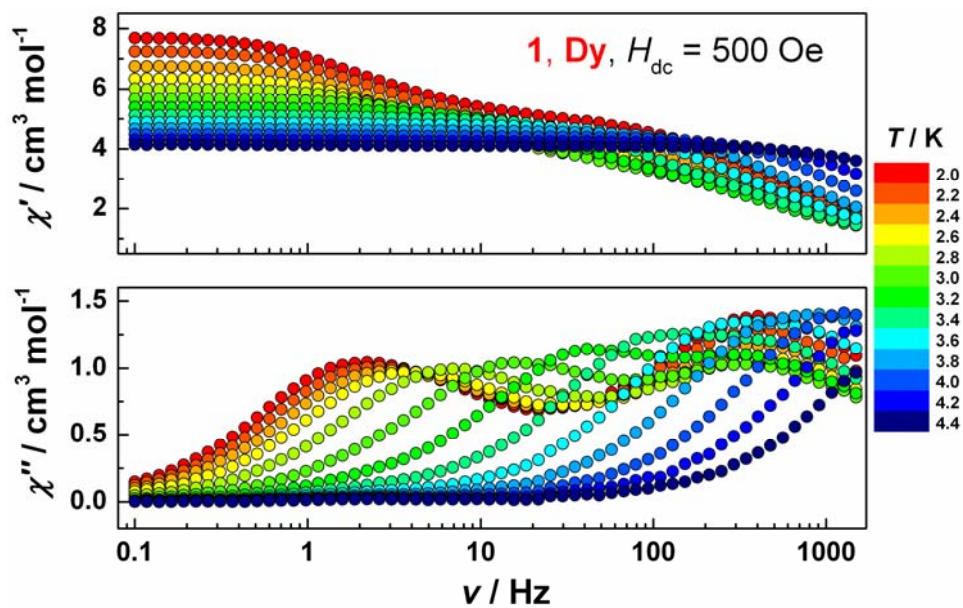


Fig. S7 Frequency dependence of the in-phase and out-of-phase ac susceptibility for **1** under 500 Oe dc field.

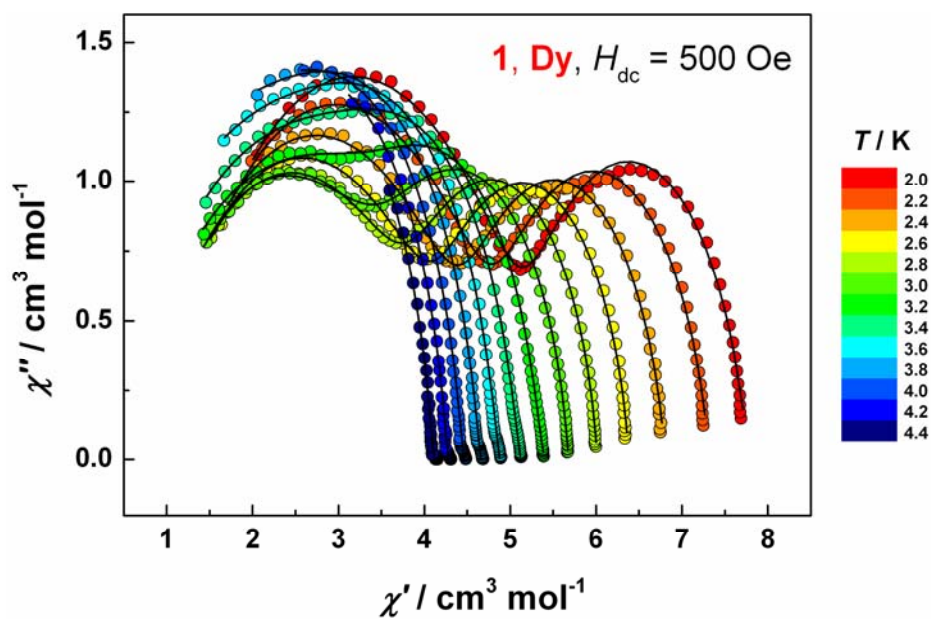


Fig. S8 Cole–Cole plots at various temperatures for **1** under 500 Oe dc field. The solid line represents a fit to the data.

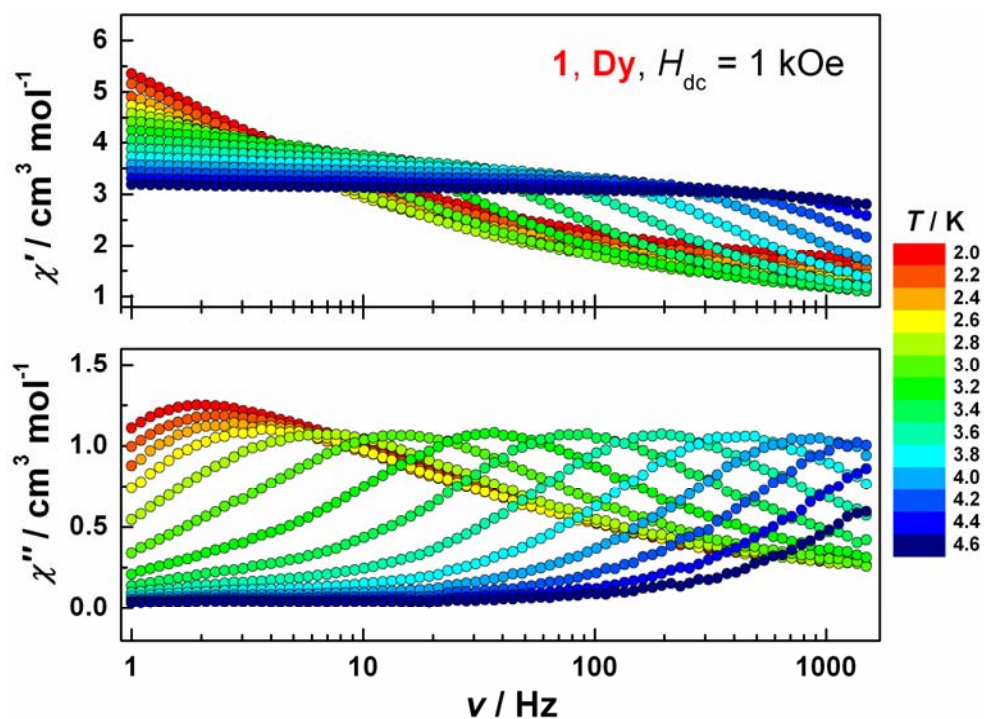


Fig. S9 Frequency dependence of the in-phase and out-of-phase ac susceptibility for **1** under 1 kOe dc field.

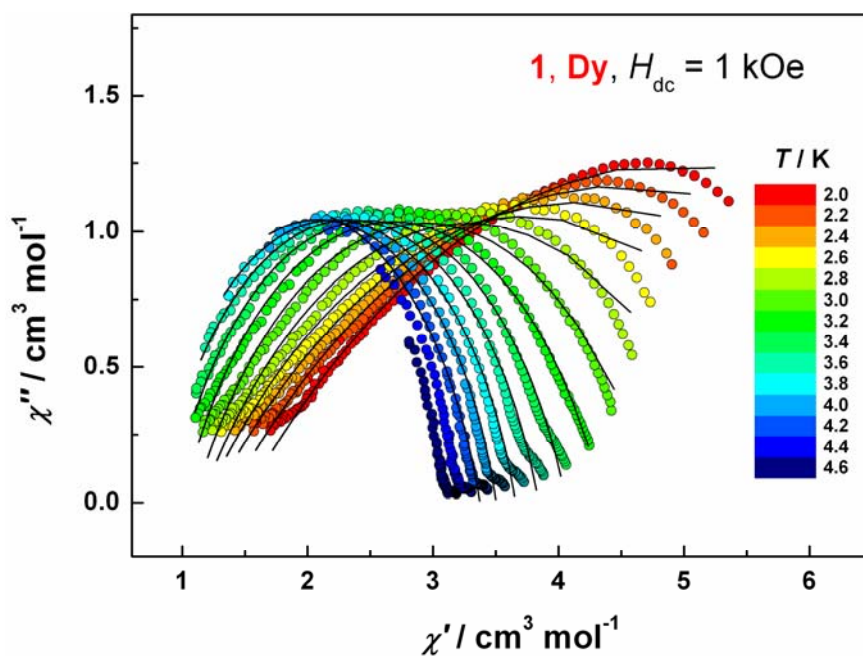


Fig. S10 Cole–Cole plots at various temperatures for **1** under 1 kOe dc field. The solid lines represent fitting with a generalized Debye model.

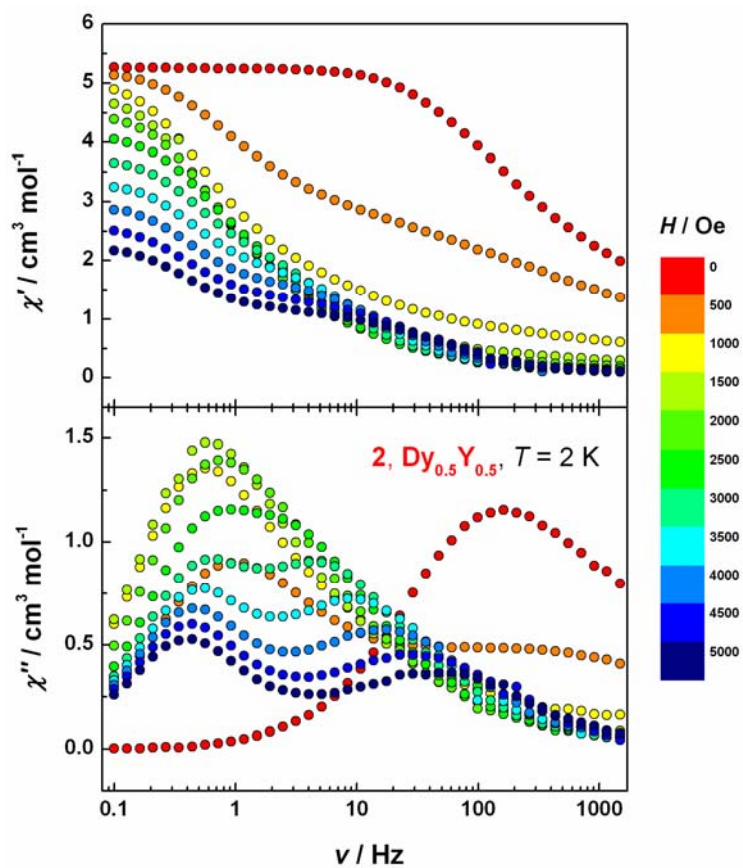


Fig. S11 Frequency dependence of the ac susceptibility for **2** at 2 K under various dc fields.

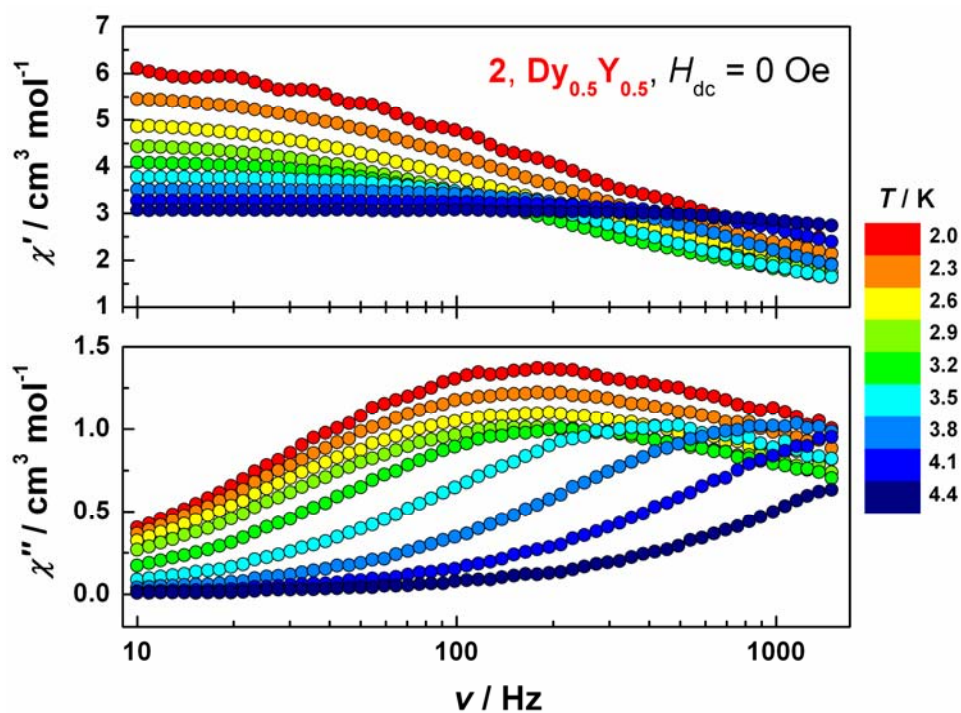


Fig. S12 Frequency dependence of the in-phase and out-of-phase ac susceptibility for **2** under 0 Oe dc field.

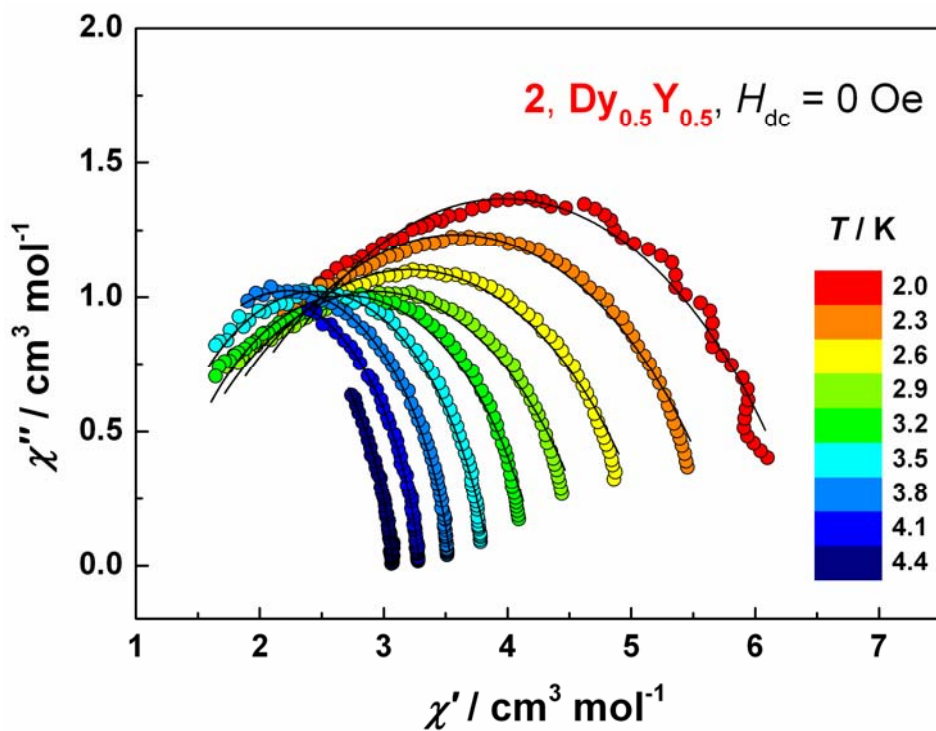


Fig. S13 Cole–Cole plots at various temperatures for **2** under 0 Oe dc field. The solid lines represent fitting with a generalized Debye model.

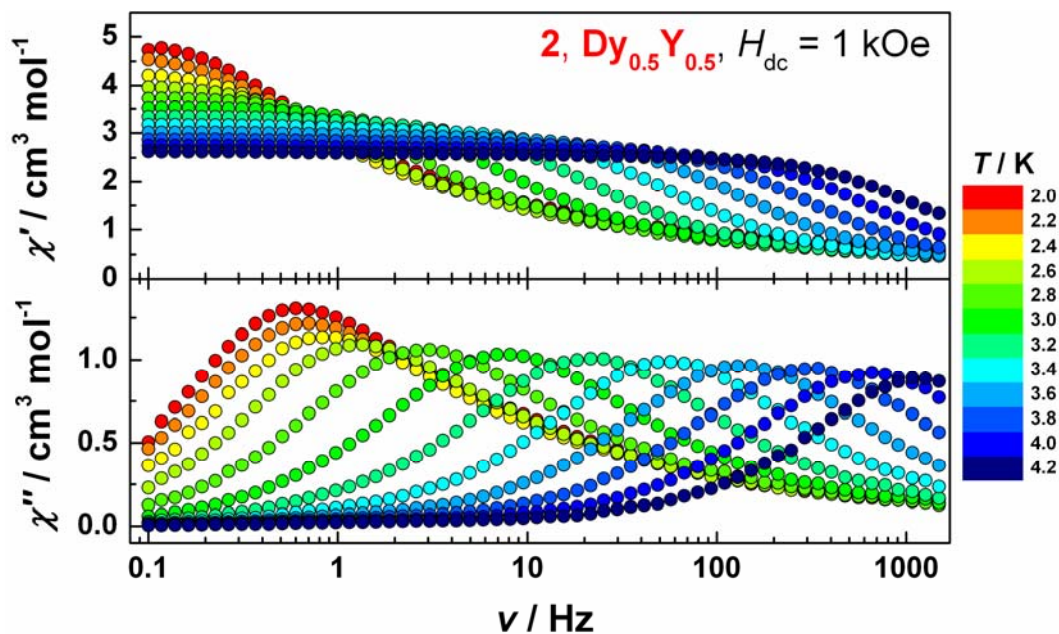


Fig. S14 Frequency dependence of the in-phase and out-of-phase ac susceptibility for **2** under 1 kOe dc field.

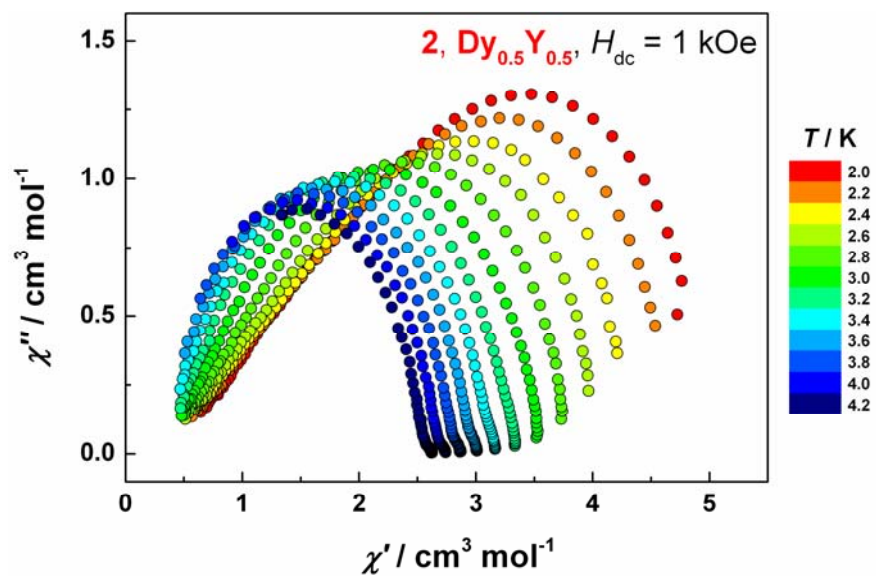


Fig. S15 Cole–Cole plots at various temperatures for **2** under 1 kOe dc field.

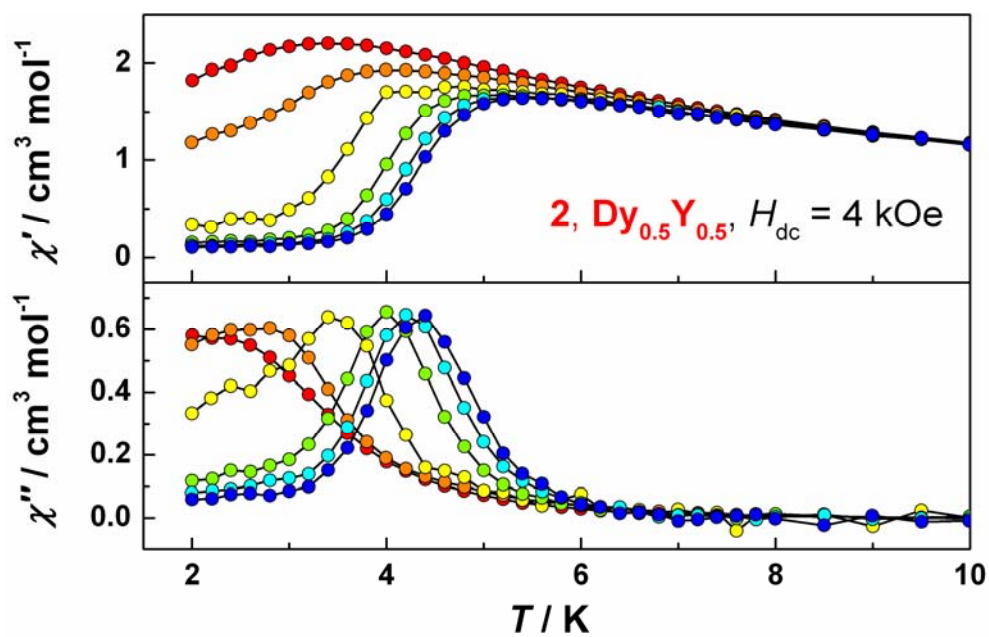


Fig. S16 Temperature dependence of the in-phase and out-of-phase ac susceptibility for **2** under 4 kOe dc field in range of 1 Hz (red) to 1500 Hz (blue).

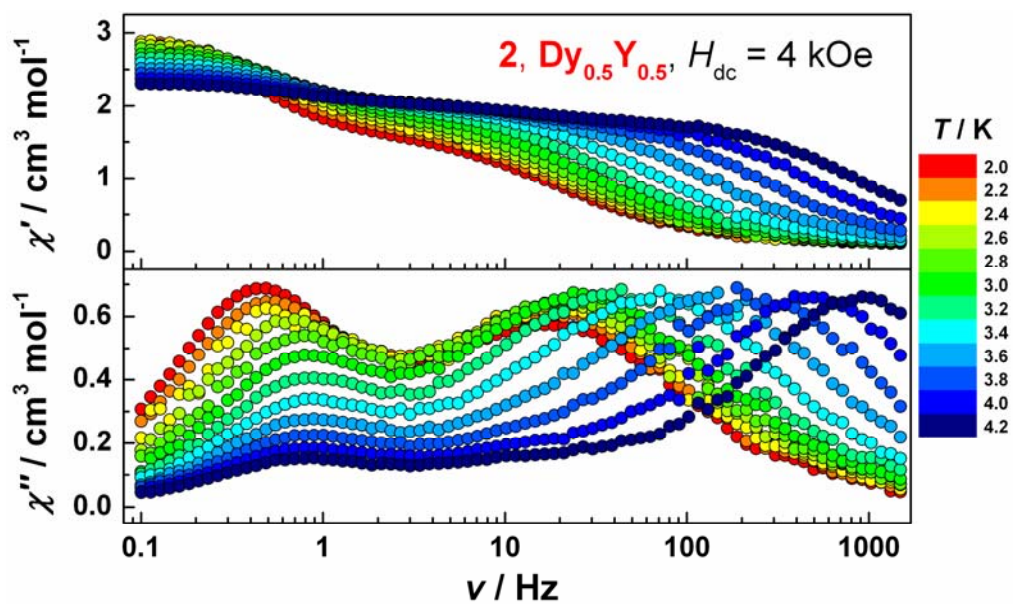


Fig. S17 Frequency dependence of the in-phase and out-of-phase ac susceptibility for **2** under 4 kOe dc field.

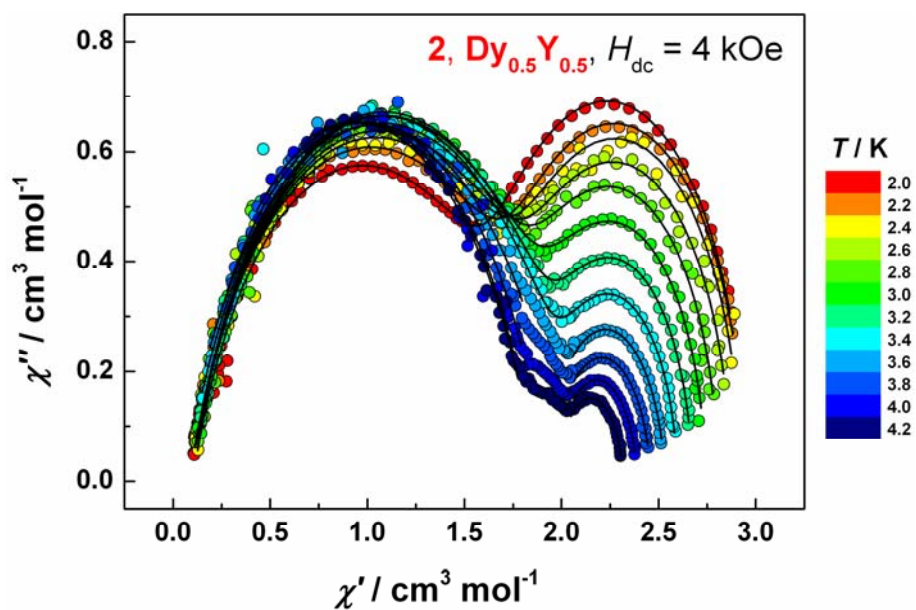


Fig. S18 Cole–Cole plots at various temperatures for **2** under 4 kOe dc field. The solid line represents a fit to the data.

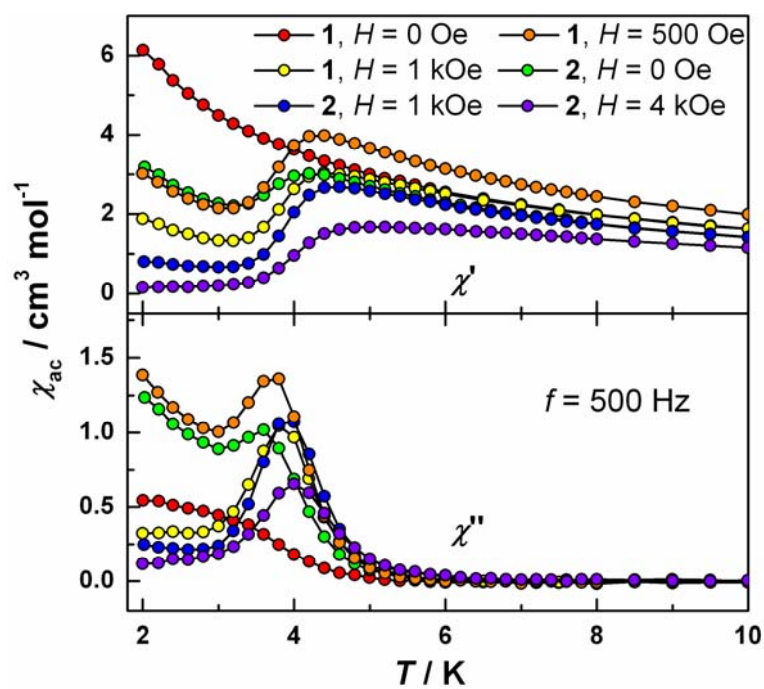


Fig. S19 Temperature dependence of the in-phase and out-of-phase ac susceptibility at 500 Hz for **1** and **2** under a number of applied dc fields.